Age Decline in the Activity of the Ca^{2+}-sensitive K^+ Channel of Human Red Blood Cells

Teresa Tiffert,[1] Nuala Daw,[1] Zipora Etzion,[2] Robert M. Bookchin,[2] and Virgilio L. Lew[1]

[1]Department of Physiology, Development and Neuroscience, University of Cambridge, Downing Street, Cambridge CB2 3EG, UK
[2]Department of Medicine, Albert Einstein College of Medicine, Bronx, NY 10461

The Ca^{2+}-sensitive K^+ channel of human red blood cells (RBCs) (Gardos channel, hIK1, hSK4) was implicated in the progressive densification of RBCs during normal senescence and in the mechanism of sickle cell dehydration. Saturating RBC Ca^{2+} loads were shown before to induce rapid and homogeneous dehydration, suggesting that Gardos channel capacity was uniform among the RBCs, regardless of age. Using glycated hemoglobin as a reliable RBC age marker, we investigated the age–activity relation of Gardos channels by measuring the mean age of RBC subpopulations exceeding a set high density boundary during dehydration. When K^+ permeabilization was induced with valinomycin, the oldest and densest cells, which started nearest to the set density boundary, crossed it first, reflecting conservation of the normal age–density distribution pattern during dehydration. However, when Ca^{2+} loads were used to induce maximal K^+ fluxes via Gardos channels in all RBCs (F_{max}), the youngest RBCs passed the boundary first, ahead of the older RBCs, indicating that Gardos channel F_{max} was highest in those young RBCs, and that the previously observed appearance of uniform dehydration concealed a substantial degree of age scrambling during the dehydration process. Further analysis of the Gardos channel age–activity relation revealed a monotonic decline in F_{max} with cell age, with a broad quasi-Gaussian F_{max} distribution among the RBCs.

The Journal of General Physiology

INTRODUCTION

A Ca^{2+}-sensitive K^+ channel (Gardos channel, hIK1, or hSK4) is expressed in the plasma membrane of human red blood cells (RBCs) (Gardos, 1958; Ishii et al., 1997; Vandorpe et al., 1998; Hoffman et al., 2003). At saturating intracellular Ca^{2+} concentrations, Gardos channel activation increases the mean K^+ flux through the plasma membrane by three orders of magnitude (Gardos, 1958; Simons, 1976; Lew and Ferreira, 1978), causing the loss of an alkaline, hypertonic effluent containing KCl and KOH (Lew and Bookchin, 1986; Freeman et al., 1987). Gardos channel activation plays an important role in the mechanism of sickle cell dehydration (Lew and Bookchin, 2005a) and may also participate in the physiological densification of aging RBCs (Clark, 1988; Lutz, 1988).

Early estimates of the number of Gardos channels per cell described values ranging from 1 to 200, with claims of wide differences among RBC subpopulations (Lew et al., 1982; Grygorczyk and Schwarz, 1983, 1985; Grygorczyk et al., 1984; Alvarez and García-Sancho, 1987; Wolff et al., 1988; Brugnara et al., 1993; Lew et al., 2004, 2005). However, when Ca^{2+} ionophores were used to induce rapid and uniform Ca^{2+} loads (Simonsen et al., 1982), triggering instant and maximal Gardos channel activation in all the cells (F_{max} at saturating Ca^{2+} loads), the distribution of dehydration rates in the RBC population, as followed by flow cytometry, proceeded to lower mean volumes with no significant variation in standard deviation or appearance of multimodality (Lew et al., 2005). This suggested uniformity of RBC dehydration rates following maximal Gardos channel activation. The discrepant estimates of the early experiments were attributed to unrecognized differences in intracellular RBC Ca^{2+} concentrations due to cell to cell variations in Ca^{2+} pump-leak balance (Lew et al., 2003, 2005). We use F_{max} throughout to represent the experimental condition in which saturating Ca^{2+} loads maximally activate the K^+ fluxes via Gardos channels in each RBC in any given sample of RBCs. Thus defined, F_{max} equals the nP_of product, where n represents the number of active Gardos channels per cell, P_o is the open state probability condition of the channels in each cell, and f is the unit channel flux at saturating Ca^{2+} levels, as determined by single channel conductance.

The apparent uniformity of Gardos channel capacity among the RBCs was surprising because it did not reveal the expected decrease in driving force for dehydration among the aging, denser RBCs, which would be seen as a tail of slower dehydrating cells in the migrating Gaussian curves. Age-dependent changes in RBC metabolism, composition, and transport have been well documented (Beutler, 1985; Lutz et al., 1988; Chasis et al., 1989; Mohandas and Groner, 1989; Romero and Romero, 1997; Boas et al., 1998; Lew et al., 2003; Kuypers and de Jong, 2004; Arese et al., 2005). The unexpected finding that Gardos channel activity appeared uniform,

Correspondence to Teresa Tiffert: jtt1000@cam.ac.uk

Abbreviations used in this paper: DEP, diethylphthalate; Hb A1c, glycated hemoglobin; Hct, hematocrit; RBC, human red blood cell.

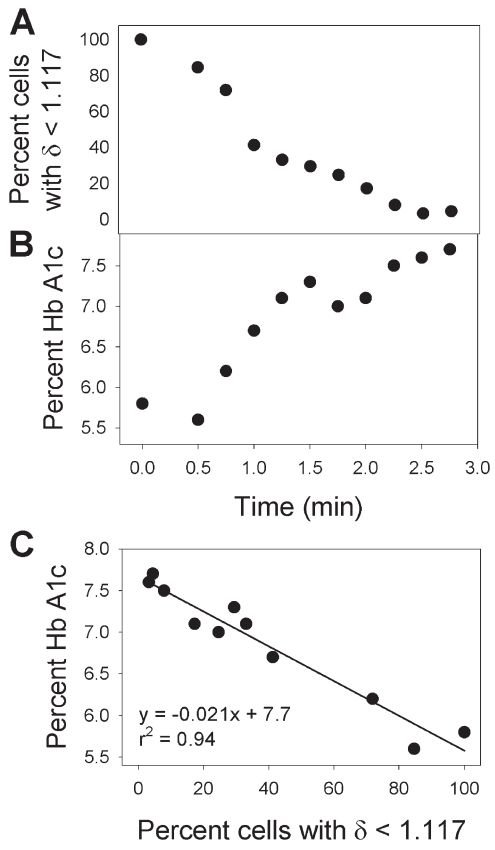

Figure 1. Relation between Hb A1c content and percent of cells harvested above diethylphthalate oil ($\delta < 1.117$ g/ml) during Gardos channel–mediated dehydration. Time = 0 in A and B corresponds to the onset of the Ca^{2+} load by addition of the ionophore A23187. As the RBCs dehydrate, the fraction recovered above the oil decreases (A), but its mean Hb A1c increases (B). Using "Time" as the parametric variable, the Hb A1c content is plotted as a function of yield in C, which also gives the parameter values of the linear regression fit through the experimental points. The results are typical of three experiments performed with blood from three donors.

regardless of RBC age, was puzzling and prompted a re-evaluation. To further investigate possible age variations in Gardos channel F_{max} among the cells, we used glycated hemoglobin (Hb A1c) as an age marker for RBCs from normal, nondiabetic subjects (Bookchin and Gallop, 1968; Bunn et al., 1976; Bosch et al., 1992).

MATERIALS AND METHODS

Experimental Design and Procedure

To detect age-related variations in Gardos channel activity among RBCs, we designed experimental conditions in which the RBC dehydration rates were determined by the Gardos channel F_{max} and by the driving gradient for dehydration in each cell, and the relative ages of the fastest and slowest dehydrating RBCs were assessed by measuring their Hb A1c contents.

Venous blood anticoagulated with EGTA was obtained from healthy donors after informed written consent. The RBCs were washed thrice in medium A containing (in mM) NaCl, 142; KCl, 3; Na-HEPES, 10, pH 7.5 at 37°C; $MgCl_2$, 0.15, and suspended at 10% hematocrit (Hct) in medium A containing 0.05 mM $CaCl_2$ and in which 10 mM NaCl was replaced by NaSCN. This low concentration of SCN^- was sufficient to bypass the rate-limiting effects of Cl^- permeability on dehydration (García-Sancho and Lew, 1988; Tiffert et al., 2001) so that the RBCs' dehydration rates were determined mainly by their Gardos channel F_{max}. The suspension was incubated at 37°C under continuous magnetic stirring and divided into equal aliquots that were processed every 15, 20, or 30 s in the different experiments. The ionophore A23187 was added at $t = 0$ to a final concentration of 10 μM in each of the aliquots to generate an instant, uniform, and saturating $[Ca^{2+}]_i$ load in all the RBCs. At the final set time for each aliquot, 1 mM EGTA was added to extract all RBC Ca^{2+}, which promptly inactivated the Gardos channels and arrested further dehydration. The EGTA-treated aliquots were dispensed into microfuge tubes containing diethylphthalate oil (DEP oil, $\delta = 1.117$ g/ml), and spun at 10,000 *g* for 1 min to separate the RBCs that exceeded that density at each time interval after Gardos channel activation. The RBCs harvested from the pellets and from the top of the oil were analyzed for hemoglobin (Hb) to estimate the proportion of RBCs recovered from each fraction, and for Hb A1c by HPLC as follows.

The Hb concentration in the RBC lysates was determined by light absorption at 415 nm (the Soret band) using a plate reader (Spectramax 190, Molecular Devices). The Hb yields of the density-segregated cell fractions were expressed as a percent of the total Hb in the unfractionated sample. Hb A1c was measured on code-labeled samples by ion exchange HPLC (Abraham et al., 1984; Bosch et al., 1992) at the Biochemistry Laboratories, Addenbrooke's Hospital, Cambridge, UK (Project 719) and at Jacobi Medical Center, Bronx, NY, using Variant II instruments (Bio-Rad Laboratories). Reproducibility of the measurements was estimated on 20 aliquots of a single blood sample, whose mean ± standard deviation was 5.71% ± 0.02, giving a coefficient of variation of 0.35%. Thus the intrinsic measurement error of the reported Hb A1c values was within the size of the points in the figures below.

In selected experiments the RBC Na^+ content was measured by flame photometry (Corning 455). The cells were washed three times in 10 volumes of isotonic $MgCl_2$, lysed, and diluted in distilled water to the required optimal reading range and measured against standards with similar Na^+ concentrations. Additional experiments on valinomycin-treated RBCs are detailed in the Results. The osmotic fragility measurements for the experiments reported in Fig. 3 below were performed as previously described (Lew et al., 1995; Raftos et al., 1996; Raftos et al., 1997). In brief, pairs of 96-well plates were used, one of each pair having a U-shaped well bottom, and the other flat bottomed for optical density measurements. Each row of the U-bottomed plate contained 250 μl each of 12 lysis media solutions with different osmolarities, ranging from 1.0 to 0.01 relative tonicity (RT) units, prepared by mixing appropriate volumes of one solution containing 149 mM NaCl and 2 mM Na-HEPES (pH 7.5 at 20°C), and a second solution containing only 2 mM of Na- HEPES (pH 7.5 at 20°C). 15 s before each sampling time, 0.5 ml of cell suspension was transferred to a groove in a plastic incubation tray (Accutran disposable incubation tray, Schleicher & Schuell) at room temperature. At the exact sampling time, a 12-channel pipette (Finnpipette, Lab Systems) was used to deliver 10-μl samples of the suspension in the incubation tray to the row of 12 wells on a U-bottomed 96-microwell plate containing the 250 μl of the lysis media, and rapidly mixed by repeated vigorous squirts with the multichannel dispenser. Each timed sample generated a full osmotic fragility curve. To estimate the fraction of hemolysis in each well, the plate was centrifuged for 5 min at 1,500 *g*, 150-μl samples of the supernatants were transferred with a 12-channel dispenser to the correspondingly labeled row on the flat-bottomed plate. The concentrations of Hb were measured on the SPECTRAmax plate

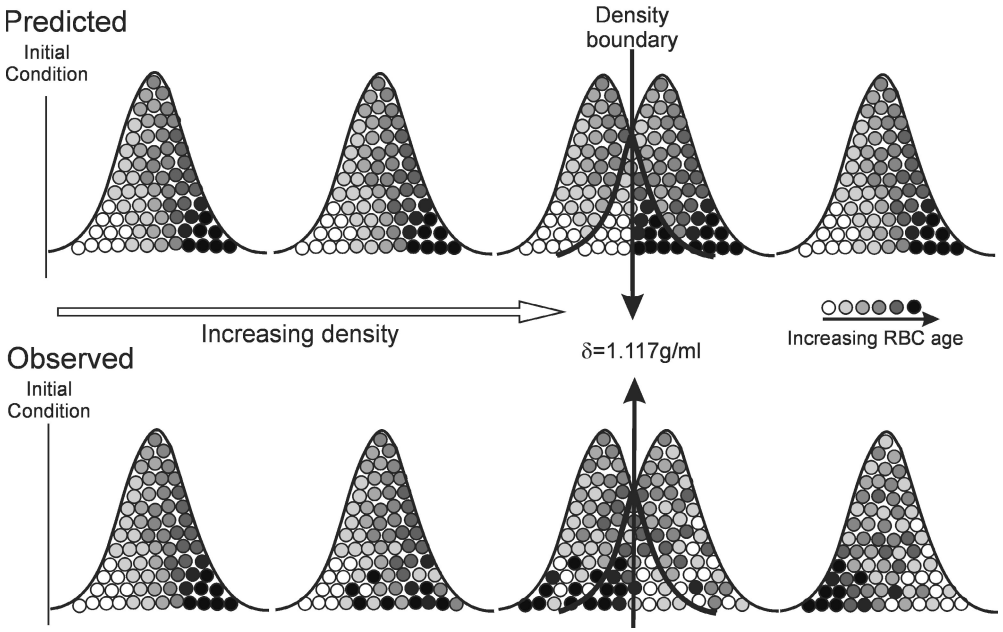

Figure 2. Diagram to illustrate the discrepancy between predicted and observed RBC age distribution during Ca^{2+}-induced dehydration. The Gaussian curves surround RBC populations (circles) of differing age, represented by the grayscale progression from white (youngest) to black (oldest). The x axis shows increasing density from left to right, and the vertical arrow shows the position of the 1.117 g/ml density boundary chosen for our experiments. Prior to Gardos channel activation, the initial RBC density distribution is represented as determined by age (the lighter young cells on the left and the denser older cells on the right). After K^+ permeabilization, the RBCs dehydrate and their increasing density is represented by the shift to the right of the Gaussian curves. The standard deviation is shown conserved representing previous experimental results (Bookchin et al., 2000; Lew et al., 2005). Those findings led to the suggestion (Predicted) that dehydration rates were similar in all the RBCs, with conservation of the original RBC age distribution within the migrating Gaussians (Predicted). The present results showed that this pattern is valid only with valinomycin-induced K^+ permeabilization. By contrast, for Gardos channel–mediated K^+ permeabilization, the results suggest that conservation of the standard deviation conceals a substantial degree of age scrambling within the migrating Gaussian curves (Observed), with the younger RBCs passing the older cells that started as most dense in the "Initial condition"; thus the RBCs that first pass the set density boundary are much younger than those reaching it last, reflecting a declining pattern of Gardos F_{max} with RBC age.

reader at the Soret band (415 nm) to calculate the percent hemolysis in each well. This was plotted as a function of relative tonicity for the osmotic fragility curves reported in Fig. 3.

RESULTS

Fig. 1, typical of three similar experiments, reports the time-dependent changes in RBC fraction and Hb A1c content of the RBCs recovered above the DEP oil after the onset of the Ca^{2+} load. As the fraction of RBCs remaining above the oil declined (Fig. 1 A), their Hb A1c fraction increased (Fig. 1 B). Fig. 1 C shows that there was an inverse correlation between the percent Hb A1c and the fraction of cells with density <1.117, indicating that those RBCs slowest to become dense had the highest Hb A1c values.

The results in Fig. 1 are in striking contrast with those expected from the known age–density distribution of RBCs, and from the assumption that RBCs of all ages would have comparable Gardos channel F_{max} activity, which would have been the simplest explanation of the observed conservation of the volume distribution profile during dehydration (Lew et al., 2005). If that explanation had been valid, then during Gardos channel–mediated dehydration, the RBCs expected to exceed the oil density first would have been the densest and oldest cells nearest to the density boundary (Fig. 2, Predicted). The observed pattern (Fig. 1) was the opposite; the youngest RBCs became dense first and the oldest RBCs last. These results suggest that RBC Gardos channel activity is not uniform, but rather that it declines with cell age.

A close analysis of the factors influencing the age distribution of Gardos-dehydrating RBCs suggests alternative possibilities. Three main factors determine the speed at which K^+-permeabilized RBCs will traverse the high-density boundary in our experiments (δ = 1.117 g/ml): (1) the initial density of each RBC determines its starting distance to the density boundary, (2) the strength of the K^+ gradient provides the driving force for dehydration, which is progressively weaker the higher the individual cell's Na^+/K^+ concentration ratio, which increases with cell age (Bookchin et al., 2000), and (3) the magnitude of the Gardos channel F_{max} in each cell. Therefore, the slower dehydration rate of the dense, aged RBCs could result from either a decreased driving force for dehydration, decay in Gardos channel F_{max}, or both.

To discriminate between the contributions of ion gradient dissipation and of Gardos channel F_{max} to the observed pattern of RBC dehydration, we sought first to subject the RBCs to a uniform, high K^+ permeability, bypassing Gardos channel activation. Under these conditions, any age-determined differences in dehydration rate could be attributed solely to the initial RBC densities

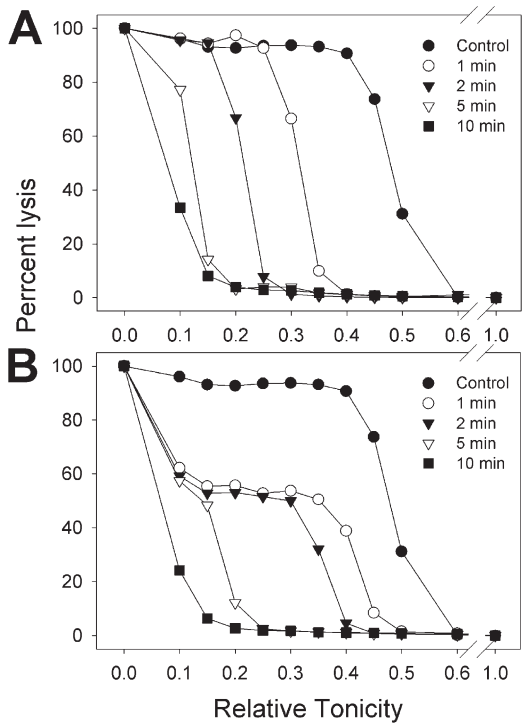

Figure 3. Evidence for uniform K^+ permeabilization induced by valinomycin in RBCs. (A) Control condition: valinomycin was added at $t = 0$ to a 10% RBC suspension in medium A (final concentration = 10 μM). The suspension was incubated at 37°C under continuous magnetic stirring, and samples for osmotic fragility curves were taken at the times indicated. The parallel displacement of the osmotic fragility curves to the left reflect uniformity of dehydration rates. (B) Valinomycin redistribution rate: an aliquot of thoroughly washed, packed RBCs from the control suspension of valinomycin-treated, fully dehydrated RBCs was added at t=0 to a 5% Hct suspension of untreated RBCs in medium A at 37°C and under magnetic stirring, giving a final Hct of 10%. The ~50% untreated RBCs in the mixed suspension dehydrated to the same final condition as the control cells at a rate similar to that of the original population (A), indicating a very rapid redistribution of valinomycin between treated and untreated RBCs. The results are representative of two experiments with blood from two donors.

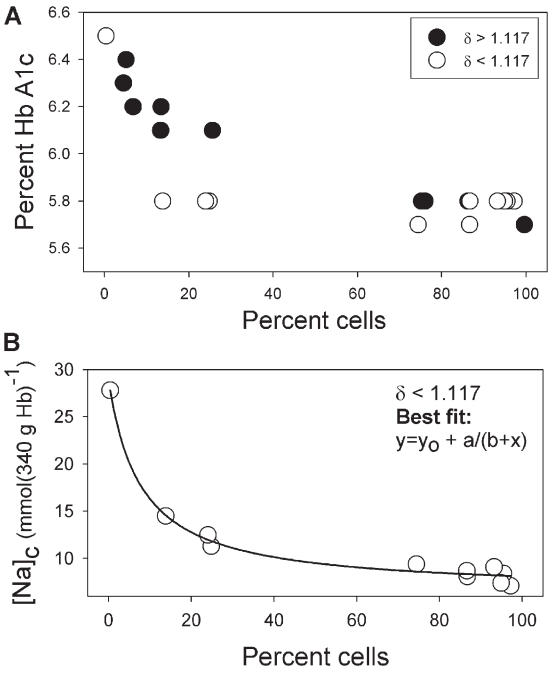

Figure 4. Hb A1c and Na^+ content of density-segregated RBCs during valinomycin-induced dehydration. A 10% RBC suspension in medium A at 37°C was treated with 10 μM valinomycin at $t = 0$. Samples were spun through diethylphthalate at frequent time intervals, and the RBCs harvested from the top and bottom of the oil were assayed for Hb (to determine yield), percent Hb A1c, and Na^+ content ($[Na]_c$). The results are typical of three experiments with blood from two donors. (A) Percent Hb A1c is plotted as a function of the percent of cells recovered from pellets (filled circles, $\delta > 1.117$) or from above the oil (open circles, $\delta < 1.117$) in timed samples after the addition of valinomycin to the cell suspension. (B) The Na^+ content of the RBCs is plotted as a function of the percent of cells recovered above the DEP oil ($\delta < 1.117$). The coefficients of the best-fit curve are $y_o = 6.50$, $a = 175$, and $b = 7.84$.

and to cell-to-cell differences in driving gradient for dehydration, not to variations in induced K^+ permeability among the RBCs.

Valinomycin, a K^+-selective ionophore (Harris and Pressman, 1967; Mueller and Rudin, 1967), has been extensively used to increase the K^+ permeability of cell membranes, but for our purposes it was necessary to establish first whether the valinomycin-induced K^+ permeability was uniform among the RBCs. If it could be shown that valinomycin rapidly equilibrated between treated and untreated RBCs, this would indicate that valinomycin distributes itself rapidly and in equal concentration per unit RBC membrane area, thus generating a uniform K^+ permeability among the RBCs. To investigate this point, we mixed valinomycin-treated with untreated RBCs, and followed the dehydration response in the mixture using the profile migration method, in which the uniformity of the RBC dehydration is monitored by the extent of slope conservation during the left-shifted displacement of the osmotic fragility curves (Raftos et al., 1996). Fig. 3 A, the control condition, shows the fairly rapid and parallel displacement of the osmotic fragility curves generated by valinomycin addition to a suspension of RBCs in low-K^+ media, as expected from uniformity of dehydration rates. Whether this uniformity was indeed the result of uniform K^+ permeabilization was explored in the condition shown in Fig. 3 B. Comparison of the dehydration rates in Fig. 3 (A and B) shows that the ~50% untreated RBCs in the mixed suspension dehydrated to the same final condition at a slower rate than that of the control RBCs but still sufficiently fast to secure a rapid redistribution of valinomycin between treated and untreated RBCs, thus ensuring uniform K^+ permeabilization among valinomycin-exposed RBCs.

Valinomycin could thus be applied to test the extent to which age-related differences in RBC dehydration

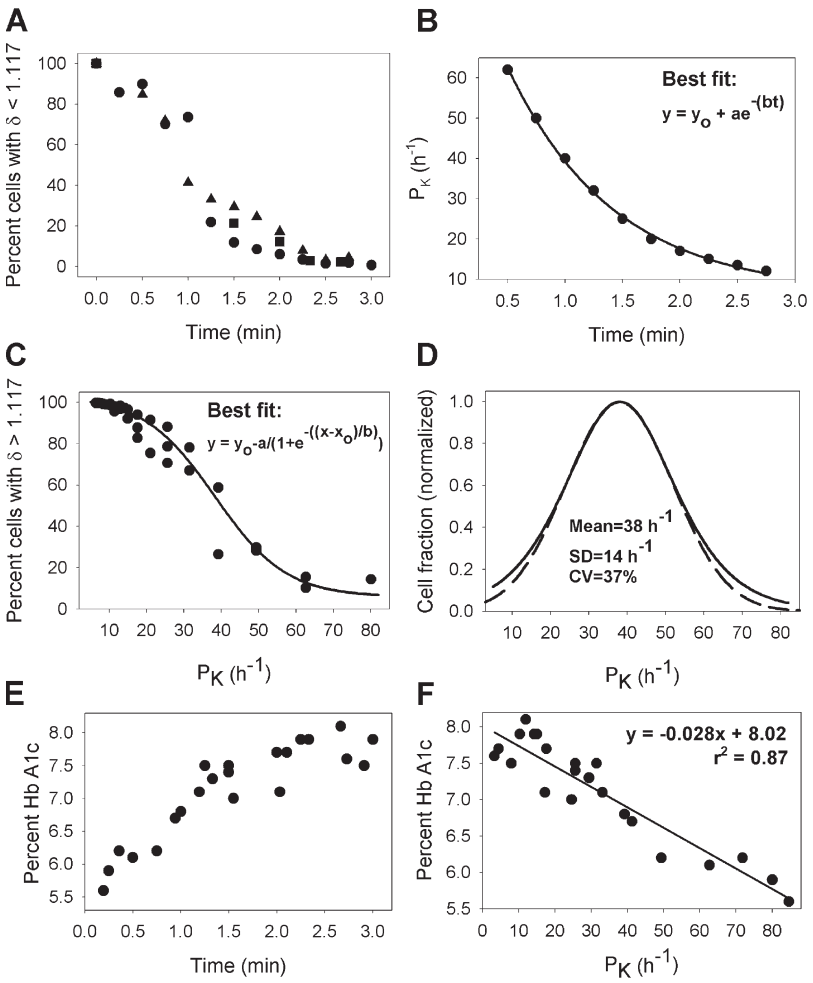

Figure 5. Distribution of Gardos channel V_{max} in RBCs and its relation with RBC age. (A) The percent RBCs recovered from the top of the DEP oil as a function of time after a saturating Ca^{2+} load. The different symbols correspond to results from three experiments with blood from three donors. The protocol was identical to that in Fig 1. (B) The Lew-Bookchin red cell model (Lew and Bookchin, 1986) was used to estimate the time needed for RBCs with different K^+ permeabilities (P_K) to exceed a density of 1.117 g/ml in conditions simulating the experiments in A. Note that P_K here corresponds to the Gardos channel F_{max}. The coefficients of the best-fit curve are y_o = 6.51, a = 96.3, and b = 1.08. (C) Using the best fit curve of B, and "Time" as the parametric variable, the combined experimental points in A were redrawn as a function of P_K from B. Note the choice of axis reorientation: "Percent cells with $\delta > 1.117$" instead of with $\delta < 1.117$ as in A plotted as a function of increasing P_K. The coefficients of the best-fit curve are y_o = 2.68, a = 105, x_o = 36.3, and b = −11.4. This curve represents the integral of the distribution of Gardos channel activity in the RBC population. (D) The derivative of the best-fit curve of C is plotted as a function of P_K, with a normalized scale for the "Cell fraction." Superimposed on the derivative curve is a Gaussian curve fit (dashed line) with the indicated statistical parameters. (E) Age–activity relation; the percent Hb A1c measured in the RBCs harvested from the top of DEP (A) as a function of time. (F) Using "Time" as the parametric variable, the percent Hb A1c in the RBCs from E is plotted as a function of P_K, from B.

rates result from their initial density distribution or from differences in their driving K^+ gradients. Fig. 4 A shows that the first RBCs to enter the pellets (filled circles, lower yields) had relatively high Hb A1c contents. These are the fastest dehydrating cells in the presence of valinomycin and must contain a considerable proportion of aged RBCs, a trend opposite to that observed with Gardos-dehydrated RBCs (Fig. 1). Comparison of the range of Hb A1c values in Fig. 1 B and Fig. 4 A shows a much narrower variation among the valinomycin-treated cells than among the Ca^{2+}-loaded cells, a consistent observation in all the experiments of this series. This indicates a more substantial age mix in the fractions recovered from valinomycin-treated RBCs than from those dehydrated by Gardos channel activation.

The Hb A1c of the RBCs above the oil (open circles) did not differ significantly from the mean values, in any of the three experiments of this series, except for a tiny RBC fraction recovered after maximal dehydration (Fig. 4 A, empty symbol at the lowest yield). The latter RBCs also had the highest Na^+ content (Fig. 4 B), sufficient to lower the driving gradient to an extent that they would not dehydrate beyond the 1.117 g/ml density boundary. The yield of these high-Na^+ cells varied from 0.3 to 0.6% in the three experiments. In Fig. 1 B, at the highest yields, the mean RBC Na^+ content was 7–10 mmol(340 g Hb)$^{-1}$. At yields from 5 to 25% the mean Na^+ content was ~10 to 16 mmol(340 g Hb)$^{-1}$, indicating a minor but progressive increase in mean Na^+ content with RBC age, and consequent reduction in the driving gradient for dehydration.

These results show that for uniformly K^+-permeabilized (valinomycin-treated) RBCs, the main determinant of dehydration rate was their initial density, i.e., their initial distance from the set density boundary (Fig. 2, top). There was also a progressive contribution of Na^+/K^+ gradient dissipation, slowing the older RBCs' dehydration and thus generating a large age mix in the density-separated fractions, with reduced variations in Hb A1c. Gradient dissipation became extreme only in a minute, high-Na^+ fraction of cells. Thus, following uniform K^+ permeabilization with valinomycin, the oldest and densest cells pass the density boundary first, but because of their weaker driving force for dehydration they soon become admixed in the pellets with younger RBCs. Thus in these conditions, dehydration rates are determined by the weak opposing effects of initial density distribution and progressively reduced driving gradient,

whereas with Ca^{2+}-induced dehydration it is the variation of Gardos channel F_{max} among the RBCs that dominates the dehydration rates, generating an inverse age–density distribution (Fig. 2, bottom).

Furthermore, the experimental need of relatively high Hct (10% in our experiments) to harvest sufficient RBCs for measurements of initial and final Hb A1c and $[Na^+]$ also contributed to the larger age mix seen with valinomycin. In such concentrated cell suspensions, the net KCl loss generates a large rapid increase in the extracellular $[K^+]$, so that the faster dehydrating RBCs are driven by a higher outward K^+ concentration gradient than those slower to dehydrate. With valinomycin, the two main contributors to the rate at which dehydrating RBCs approach the density boundary are the initial cell density distribution and the strength of the driving gradient. Initial cell density places the older RBCs nearer the density boundary, but the driving gradient of the younger RBCs (which start further from the boundary) is stronger. The younger cells dehydrate faster and the K^+ they release slows the rate at which the older cells approach the boundary, thus further mixing the ages of dehydrating, valinomycin-treated RBCs relative to their original age–density distribution. With Ca^{2+}-induced dehydration, on the other hand, the rise in extracellular $[K^+]$ during dehydration amplifies their age differences in Gardos F_{max}, by further slowing the older RBCs' dehydration rates.

The protocol in Fig. 1 can now be applied to analyze the distribution of Gardos channel F_{max} among the RBCs. Fig. 5 A shows the compiled results of three experiments like that in Fig. 1. For a rough estimate of the Gardos channel F_{max} distribution, we assume that the time it takes for any RBC to reach the boundary density is determined primarily by its Gardos channel F_{max}, and that its initial density and the status of its driving gradient have negligible effects. With these assumptions, we can apply the Lew-Bookchin red cell model (Lew and Bookchin, 1986) to simulate the present experimental conditions and compute the time needed for RBCs with different K^+ permeabilities (P_K) (representing Gardos channel F_{max} variations) to attain a density of 1.117 g/ml. The simulation in Fig. 5 B plots P_K as a function of time. Using "Time" as the parametric variable, and the fit in Fig. 5 B, we can now plot cell frequency as a function of P_K from the data in Fig. 5 A, and obtain the relation shown in Fig. 5 C. The best fit empirical curve in Fig. 5 C represents the integral of the distribution of Gardos channel F_{max} among the RBCs. Its derivative, representing the distribution of Gardos channel F_{max}, is shown in Fig. 5 D. The dashed line shows the best Gaussian fit of the derivative curve, rendering a mean P_K of $\sim$38 h^{-1} and a coefficient of variation of $\sim$37%. Fig. 5 E reports the variation in Hb A1c in the RBCs recovered above the oil at the time intervals shown after the Ca^{2+} load. Again, using "Time" as the parametric variable for Fig. 5 (B and E) we can plot the percent Hb A1c as a function of P_K (Fig. 5 F); this reveals an inverse relation between percent Hb A1c and P_K corresponding to an inverse relation between RBC age and Gardos channel F_{max}.

With caution, given the simplifying assumptions inherent in this analysis and the unavoidable age mix in the samples, these results show that the Gardos channel F_{max} declines monotonically with RBC age (Fig. 5, E and F), and that the F_{max} values among the RBCs follows a fairly broad, approximate Gaussian distribution (Fig. 5 D) with a very high mean P_K. It is important to note that even the lowest P_K value in the oldest RBCs is $\sim$10 h^{-1}, still three to four orders of magnitude above the ground K^+ permeability of the human RBC (Beaugé and Lew, 1977; Lew and Beaugé, 1979).

DISCUSSION

The present results show that Gardos channel activity, measured at saturating Ca^{2+} loads, declines sharply throughout the lifespan of human RBCs. However, these results do not allow us to discriminate between the separate contributions of n or P_o to the age decline in Gardos channel F_{max}. A reduction in n only is equivalent to a cumulative and progressive all-or-none inactivation of Gardos channels within each cell. Such an all-or-none type of inactivation was observed experimentally with the Ca^{2+}-Mg^{2+}-ATPase of isolated RBC membranes exposed to high glucose concentrations (Gonzalez Flecha et al., 1999). These authors showed that glycation of a single essential Lys residue, probably located near the catalytic ATP site of the ATPase, caused full inhibition, whereas those molecules without glycation of the vulnerable Lys residue remained functionally normal. The possible effects of glycation on Gardos channel function have not yet been explored. A reduction in P_o with cell age may perhaps be inferred from the peculiar temperature response of the Gardos channels observed in excised membrane patches from RBC membranes (Grygorczyk, 1987). At saturating Ca^{2+} levels, P_o was shown to fall sharply, by >90%, when the temperature was increased from 30°C to 35°C. On the other hand, when Gardos channel–mediated K^+ fluxes were measured in intact RBCs, the fall in efflux rate constant between 27°C and 37°C was only about half (Hoffman et al., 2003). Hoffman et al. (2003) considered the possibility that this discrepancy in the magnitude of the temperature effect may result from heterogeneity in the response of intact RBC populations. Taken together with the present results, the discrepancy may be explained if what has been detected as a differential temperature effect reflects in fact a decline in P_o with RBC age. In this interpretation, the P_o of young RBCs would be high and show little change with temperature. As RBCs age, their channels undergo structural or regulatory

changes that can be exposed experimentally as a progressive decline in P_o at temperatures >30°C. Thus, age heterogeneity in the RBC population would generate a mean temperature differential that could mask the extreme high and low P_o values at 37°C in young and old RBCs, respectively. This interpretation assumes that the reported patch clamp data were obtained preferentially from aged RBCs with low P_o responses at 35°C. Further research on excised patches from age-segregated RBCs is needed to investigate whether the temperature effect is related to RBC age and to assess the contribution of P_o to F_{max} decline.

To the extent that the homeostatic changes in aging RBCs are driven by elevated $[Ca^{2+}]_i$ levels, the effects of decline in Gardos channel activity and of the minor reductions in driving force for dehydration, as quantified above, would have negligible effects on age-associated densification. The pattern of Na^+ gain in aging RBCs (Fig. 4 B) suggests a slow and gradual Na^+ gain, with a sharp late increase leading to the formation of the light, high-Na^+ cells in a terminal homeostatic condition (Bookchin et al., 2000).

The effect of age-related decline in Gardos channel F_{max} may be relevant to the pattern of sickle cell dehydration (Lew and Bookchin, 2005). The interaction of the polymers of deoxygenated haemoglobin S with the membrane of sickle cells activates a poorly selective cation permeability pathway, Psickle, with a stochastic distribution of Ca^{2+} permeabilities in the RBC population in each deoxygenation event (Lew et al., 1997). The variably elevated $[Ca^{2+}]_i$ activates Gardos channels, triggering RBC dehydration and acidification. In sickle reticulocytes and young sickle cells, which retain a high activity of acid-sensitive K:Cl cotransporters (Brugnara et al., 1986), Gardos-induced acidification stimulates further K:Cl-mediated dehydration, segregating sickle cells into slow- and fast-track dehydrating cells, with a predominance of young cells in the densest fraction of sickle cells, rich in irreversible sickle cells (Bookchin et al., 1991; Lew et al., 1991). The age distribution of Gardos channel F_{max} documented here for normal RBCs reveals extraordinarily high F_{max} values in young RBCs. Young cells also have the highest driving gradients for dehydration via K^+ permeabilization. These features may contribute to the increased vulnerability of young SS cells to dehydration observed by us and others, and they provide an additional mechanism for enhancing the differences between slow- and fast-track dehydrating SS RBCs.

We thank Lynn Macdonald for excellent technical assistance and Angus Gidman for the supervision of the Hb A1c measurements in Cambridge (Addenbrooke's Hospital, Cambridge, UK; Project 719).

This work was supported by grants from the Wellcome Trust (UK) and National Institutes of Health (HL28018, HL58512 and RR12248). Approval for these studies was obtained from the Institutional Review Boards of the University of Cambridge (Cambridge, UK) and from the Albert Einstein College of Medicine (New York, NY).

Olaf S. Andersen served as editor.

Submitted: 14 February 2007
Accepted: 6 April 2007

REFERENCES

Abraham, E.C., A. Abraham, and M. Stallings. 1984. High-pressure liquid chromatographic separation of glycosylated and acetylated minor hemoglobins in newborn infants and in patients with sickle cell disease. *J. Lab. Clin. Med.* 104:1027–1034.

Alvarez, J., and J. García-Sancho. 1987. An estimate of the number of Ca^{2+}-dependent K^+ channels in the human red cell. *Biochim. Biophys. Acta.* 903:543–546.

Arese, P., F. Turrini, and E. Schwarzer. 2005. Band 3/complement-mediated recognition and removal of normally senescent and pathological human erythrocytes. *Cell. Physiol. Biochem.* 16:133–146.

Beaugé, L., and V.L. Lew. 1977. Passive fluxes of sodium and potassium across red cell membranes. *In* Membrane Transport in Red Cells. J.C. Ellory and V.L. Lew, editors. Academic Press, London. 39–51.

Beutler, E. 1985. Biphasic loss of red cell enzyme activity during in vivo aging. *Prog. Clin. Biol. Res.* 195:317–333.

Boas, F.E., L. Forman, and E. Beutler. 1998. Phosphatidylserine exposure and red cell viability in red cell aging and in hemolytic anemia. *Proc. Natl. Acad. Sci. USA.* 95:3077–3081.

Bookchin, R.M., Z. Etzion, M. Sorette, N. Mohandas, J.N. Skepper, and V.L. Lew. 2000. Identification and characterization of a newly recognized population of high-Na^+, low-K^+, low-density sickle and normal red cells. *Proc. Natl. Acad. Sci. USA.* 97:8045–8050.

Bookchin, R.M., and P.M. Gallop. 1968. Structure of hemoglobin A_{1c}: nature of the N-terminal chain blocking group. *Biochem. Biophys. Res. Commun.* 32:86–93.

Bookchin, R.M., O.E. Ortiz, and V.L. Lew. 1991. Evidence for a direct reticulocyte origin of dense red cells in sickle cell anemia. *J. Clin. Invest.* 87:113–124.

Bosch, F.H., J.M. Werre, B. Roerdinkholder-Stoelwinder, T.H. Huls, F.L. Willekens, and M.R. Halie. 1992. Characteristics of red blood cell populations fractionated with a combination of counterflow centrifugation and Percoll separation. *Blood.* 79:254–260.

Brugnara, C., H.F. Bunn, and D.C. Tosteson. 1986. Regulation of erythrocyte cation and water content in sickle cell anemia. *Science.* 232:388–390.

Brugnara, C., L. De Franceschi, and S.L. Alper. 1993. Ca^{2+}-activated K^+ transport in erythrocytes. Comparison of binding and transport inhibition by scorpion toxins. *J. Biol. Chem.* 268:8760–8768.

Bunn, H.F., D.N. Haney, S. Kamin, K.H. Gabbay, and P.M. Gallop. 1976. The biosynthesis of human hemoglobin A1c. Slow glycosylation of hemoglobin in vivo. *J. Clin. Invest.* 57:1652–1659.

Chasis, J.A., M. Prenant, A. Leung, and N. Mohandas. 1989. Membrane assembly and remodeling during reticulocyte maturation. *Blood.* 74:1112–1120.

Clark, M.R. 1988. Senescence of red blood cells: progress and problems. *Physiol. Rev.* 68:503–554.

Freeman, C.J., R.M. Bookchin, O.E. Ortiz, and V.L. Lew. 1987. K-permeabilized human red cells lose an alkaline, hypertonic fluid containing excess K over diffusible anions. *J. Membr. Biol.* 96:235–241.

García-Sancho, J., and V.L. Lew. 1988. Detection and separation of human red cells with different calcium contents following uniform calcium permeabilization. *J. Physiol.* 407:505–522.

Gardos, G. 1958. The function of calcium in the potassium permeability of human erythrocytes. *Biochim. Biophys. Acta.* 30:653–654.

González Flecha, F.L., P.R. Castello, J.J. Gagliardino, and J.P. Rossi. 1999. Molecular characterization of the glycated plasma membrane calcium pump. *J. Membr. Biol.* 171:25–34.

Grygorczyk, R. 1987. Temperature dependence of Ca^{2+}-activated K^+ currents in the membrane of human erythrocytes. *Biochim. Biophys. Acta.* 902:159–168.

Grygorczyk, R., and W. Schwarz. 1983. Properties of the Ca^{2+}-activated K^+ conductance of human red cells as revealed by the patch-clamp technique. *Cell Calcium.* 4:499–510.

Grygorczyk, R., and W. Schwarz. 1985. Ca^{2+}-activated K^+ permeability in human erythrocytes: modulation of single-channel events. *Eur. Biophys. J.* 12:57–65.

Grygorczyk, R., W. Schwarz, and H. Passow. 1984. Ca^{2+}-activated K^+ channels in human red cells. Comparison of single-channel currents with ion fluxes. *Biophys. J.* 45:693–698.

Harris, E.J., and B.C. Pressman. 1967. Obligate cation exchanges in red cells. *Nature.* 216:918–920.

Hoffman, J.F., W. Joiner, K. Nehrke, O. Potapova, K. Foye, and A. Wickrema. 2003. The hSK4 (KCNN4) isoform is the Ca^{2+}-activated K^+ channel (Gardos channel) in human red blood cells. *Proc. Natl. Acad. Sci. USA.* 100:7366–7371.

Ishii, T.M., C. Silvia, B. Hirschberg, C.T. Bond, J.P. Adelman, and J. Maylie. 1997. A human intermediate conductance calcium-activated potassium channel. *Proc. Natl. Acad. Sci. USA.* 94:11651–11656.

Kuypers, F.A., and K. de Jong. 2004. The role of phosphatidylserine in recognition and removal of erythrocytes. *Cell. Mol. Biol. (Noisy - le-grand)* 50:147–158.

Lew, V.L., and L.A. Beaugé. 1979. Passive cation fluxes in red cell membranes. *In* Transport across biological membranes. Vol. II. G. Giebisch, D.C. Tosteson, and H.H. Ussing, editors. Springer-Verlag, Berlin. 85–115.

Lew, V.L., and R.M. Bookchin. 1986. Volume, pH and-ion content regulation in human red cells: analysis of transient behavior with an integrated model. *J. Membr. Biol.* 92:57–74.

Lew, V.L., and R.M. Bookchin. 2005. Ion transport pathology in the mechanism of sickle cell dehydration. *Physiol. Rev.* 85:179–200.

Lew, V.L., and H.G. Ferreira. 1978. Calcium transport and the properties of a calcium-activated potassium channel in red cell membranes. *In* Current Topics in Membranes and Transport. Vol. 10. A. Kleinzeller and F. Bronner, editors. Academic Press, New York. 217–277.

Lew, V.L., S. Muallem, and C.A. Seymour. 1982. Properties of the Ca^{2+}-activated K^+ channel in one-step inside-out vesicles from human red cell membranes. *Nature.* 296:742–744.

Lew, V.L., C.J. Freeman, O.E. Ortiz, and R.M. Bookchin. 1991. A mathematical model on the volume, pH and ion content regulation of reticulocytes. Application to the pathophysiology of sickle cell dehydration. *J. Clin. Invest.* 87:100–112.

Lew, V.L., J.E. Raftos, M.P. Sorette, R.M. Bookchin, and N. Mohandas. 1995. Generation of normal human red cell volume, hemoglobin content and membrane area distributions, by "birth" or regulation? *Blood.* 86:334–341.

Lew, V.L., O.E. Ortiz-Carranza, and R.M. Bookchin. 1997. Stochastic nature and red cell population distribution of the sickling-induced Ca^{2+} permeability. *J. Clin. Invest.* 99:2727–2735.

Lew, V.L., N. Daw, D. Perdomo, Z. Etzion, R.M. Bookchin, and T. Tiffert. 2003. Distribution of plasma membrane Ca^{2+} pump activity in normal human red blood cells. *Blood.* 102:4206–4213.

Lew, V.L., T. Tiffert, Z. Etzion, D. Perdomo, N. Daw, L. Macdonald, and R.M. Bookchin. 2005. Distribution of dehydration rates generated by maximal Gardos-channel activation in normal and sickle red blood cells. *Blood.* 105:361–367.

Lutz, H.U. 1988. Red cell density and red cell age. *Blood Cells.* 14:76–80.

Lutz, H.U., S. Fasler, P. Stammler, F. Bussolino, and P. Arese. 1988. Naturally occurring anti-band 3 antibodies and complement in phagocytosis of oxidatively-stressed and in clearance of senescent red cells. *Blood Cells.* 14:175–195.

Mohandas, N., and W. Groner. 1989. Cell membrane and volume changes during red cell development and aging. *Ann. N. Y. Acad. Sci.* 554:217–224.

Mueller, P., and D.O. Rudin. 1967. Development of K^+-Na^+ discrimination in experimental bimolecular lipid membranes by macrocyclic antibiotics. *Biochem. Biophys. Res. Commun.* 26:398–404.

Raftos, J.E., R.M. Bookchin, and V.L. Lew. 1996. Distribution of chloride permeabilities in normal human red cells. *J. Physiol.* 491:773–777.

Raftos, J.E., R.M. Bookchin, and V.L. Lew. 1997. Measurement of the distribution of anion-exchange function in normal human red cells. *J. Physiol.* 499:17–25.

Romero, P.J., and E.A. Romero. 1997. Differences in Ca^{2+} pumping activity between sub-populations of human red cells. *Cell Calcium.* 21:353–358.

Simons, T.J.B. 1976. Calcium-dependent potassium exchange in human red cell ghosts. *J. Physiol.* 256:227–244.

Simonsen, L.O., J. Gomme, and V.L. Lew. 1982. Uniform ionophore A23187 distribution and cytoplasmic calcium buffering in intact human red cells. *Biochim. Biophys. Acta.* 692:431–440.

Tiffert, T., N. Daw, D. Perdomo, and V.L. Lew. 2001. A fast and simple screening test to search for specific inhibitors of the plasma membrane calcium pump. *J. Lab. Clin. Med.* 137:199–207.

Vandorpe, D.H., B.E. Shmukler, L. Jiang, B. Lim, J. Maylie, J.P. Adelman, L. De Franceschi, M.D. Cappellini, C. Brugnara, and S.L. Alper. 1998. cDNA cloning and functional characterization of the mouse Ca^{2+}-gated K^+ channel, mIK1. Roles in regulatory volume decrease and erythroid differentiation. *J. Biol. Chem.* 273:21542–21553.

Wolff, D., A. Spalvins, and M. Canessa. 1988. Charybdotoxin blocks with high affinity the Ca-activated K^+ channel of Hb A and Hb S red cells: individual differences in the number of channels. *J. Membr. Biol.* 106:243–252.